Computers and Concrete, *Vol. 19, No. 5 (2017) 589-597*
DOI: https://doi.org/10.12989/cac.2017.19.5.589

Reinforcement detailing of a corbel via an integrated strut-and-tie modeling approach

Fatih Mehmet Özkal[*1] and Habib Uysal[2a]

[1]*Department of Civil Engineering, Erzincan University, 24060, Erzincan, Turkey*
[2]*Department of Civil Engineering, Atatürk University, 25240, Erzurum, Turkey*

(Received October 25, 2016, Revised January 15, 2017, Accepted February 12, 2017)

Abstract. Strut-and-tie modeling method, which evolved on truss-model approach, has generally been preferred for the design of complex reinforced concrete structures and structural elements that have critical shear behavior. Some structural members having disturbed regions require exceptional detailing for all support and loading conditions, such as the beam-column connections, deep beams, short columns or corbels. Considering the general expectation of exhibiting brittle behavior, corbels are somewhat dissimilar to other shear critical structures. In this study, reinforcement layout of a corbel model was determined by the participation of structural optimization and strut-and-tie modeling methods, and an experimental comparison was performed against a conventionally designed model.

Keywords: computer-aided design; strut-and-tie model; structural optimization; performance decision; reinforced concrete; steel reinforcement

1. Introduction

Because mechanical behavior of reinforced concrete (RC) cannot be anticipated with certainty, optimal design of RC members has mostly been kept in the background by researchers. However, strut-and-tie modeling (STM) method is based on a basic assumption that disturbed (D) regions in RC members can be analyzed and designed based on the idea of assuming a truss-like structure develops in the structure and this fictive truss has frictionless pin-joints. There are two primary signs for the determination of D regions: (1) Geometrical, e.g., openings or sharp changes in the structure; and (2) Mechanical, due to the applied loads, e.g. concentrated loads (Victoria *et al.* 2011). Throughout this assumption, internal stress trajectories are regarded as the primary baseline for this load-transmitting truss, which consists of concrete struts and steel ties. However, instead of the load-path method, some optimization-based design approaches have widely been investigated in order to facilitate the determination of stress trajectories and construction of the internal truss. Recent improvements in computer technology and especially development of finite element method have been facilitating these studies every day.

The idea of using a truss model was first proposed by Ritter (1899) and Mörsch (1902) for the shear design of flexural concrete members. The publications of Collins and Mitchell (1986), Schlaich *et al.* (1987) and Cook and Mitchell (1988) are pioneer studies for the truss model approach, in some way (Qazi *et al*. 2015). The strut-and-tie model (STM) is one of the rational and relatively simple design approaches for non-flexural members, where traditional beam theory cannot be applied (Wight and Parra-Montesinos 2003). Prior to the modeling, internal forces in discontinuity regions are evaluated by considering that compression struts are concrete, tension ties are steel reinforcement and nodal zones are truss joints (MacGregor 1997, Yavuz 2016). It is based on lower bound theory of plasticity, which assumes that concrete and steel are frequently plastic at the limit state. Efficiency factors are then applied to uni-axial strength of concrete to account for concrete softening and cracking (Schlaich *et al.* 1987). Technical guidance for the assessment and design of RC members by STM method can be found in the BS 8110 (1997), Eurocode 2 (2004), CSA (2004), NZS 3101 (2006), FIB (2010), AASTHO-LRFD (2010) and ACI 318M-14 (2014) design codes at the present time (Chae and Yun 2015). Optimization studies that consisted in converting the continuous environment of an RC structure into a truss system were launched at the beginning of the 20th century. Since then, several analogy methods have improved on this idea (Özkal and Uysal 2016). Structural topology optimization method, which withstands the complexities of traditional continuous and discrete methods, has become an effective design tool for obtaining efficient and lighter structures since the pioneer work of Michell (1904) for truss theory and the seminal work of Bendsøe and Kikuchi (1988) for homogenization method (Wang *et al.* 2006). Depending on these two keystones, topology optimization algorithm was improved by Xie and Steven (1993) by evaluating the structural efficiency degree of finite elements in the design area (Özkal 2012).

Several researchers have led to the use of structural

∗Corresponding author, Assistant Professor
E-mail: fmozkal@erzincan.edu.tr
[a]Associate Professor
E-mail: huysal@atauni.edu.tr

http://www.techno-press.org/?journal=cac&subpage=8 ISSN: 1598-8198 (Print), 1598-818X (Online)

optimization techniques to facilitate the evaluation of internal stress trajectories and automate the constitution of strut-and-tie models. These studies show that the strut-and-tie modeling method, especially, is an important assistant in the purpose of integrating the topology optimization into the civil engineering field. However, most of them do not consider existing structural codes and are generally limited to the theoretical assumptions. This study suggests an integrated design approach for the determination of reinforcement layout in RC members by the structural optimization and strut-and-tie modeling methods, respectively. Afterwards, a typical corbel model is designed, produced and tested in order to compare the mechanical behavior of new approach to the conventional one.

2. Research significance

Unlike the high number of truss-system studies in the civil engineering area, the optimal design of RC structural members has mostly been kept in the background by researchers. Despite the fact that structural-optimization studies for reinforced concrete members does not attract significant attention, several theoretical studies on topology-based evolutionary structural optimization have begun to appear in recent years. However, the existence of purely theoretical studies without real material properties and structural behavior, and the absence of a detailed comparison with the other design methods exhibit the necessity of an experimental study to correlate the topology optimization with the STM method. This paper focuses on the optimum reinforcement layout design of concrete corbels in order to response this requisition.

3. Reinforcement layout design of corbels

The term “corbel” is generally restricted to cantilevers having shear span-depth ratios less than unity and jutting out from walls or columns. Such a small ratio causes the strength of corbels to often be controlled by shear, which is similar to deep beams (Hwang *et al.* 2000). They are generally preferred to support prefabricated beams or floors at building joints by transmitting internal forces to the vertical structural members. These structural members are primarily designed to resist the ultimate shear force applied to them by the beam, and the ultimate horizontal action due to beam shrinkage, creep, or temperature changes (Russo *et al*. 2006). The principal failure modes for members without stirrups are: 1) shear failure; 2) yielding of the principal reinforcement (flexural tension); 3) crushing of concrete strut (flexural compression); and 4) diagonal splitting (Kriz and Raths 1965, Mattock *et al*. 1976, Russo *et al.* 2006). Experimental observations have revealed several scenarios of corbel failure, which are presented in Fig. 1 and explained below by Celep and Kumbasar (2005).

(a) Inadequate overlap length of the top rebar will cause the front part of corbel to crack and split off.

(b) If the bearing plate under the external load is very small, concrete beneath the plate will crush.

(c) If the external load is close to the edge of the corbel, outer part of concrete will split off.

(d) Shear effect on column’s face causes inclined cracks. Merger of these cracks will split the corbel from the column.

(e) Tensile stresses in the corbel will cause inclined cracks and after then concrete strut will crush.

(f) Following the horizontal tension rebar’s yield and excessive strain arising from bending moment, cracks will occur and expand on column’s face. Subsequently, concrete strut will crush and the corbel will collapse.

In this study, corbel model in Fig. 2 was evaluated based on two methods according to a vertical load of 100 kN. First model (C1) was designed according to the instructions of national TS 500 (2000) code while the other model (C2) was designed by the new integrated design approach especially according to the instructions of codes containing STM method. Reinforcement design of columns for both of the models is identical and calculated within the conventional procedure. It is important to note that both of the models were designed in accordance with the materials property limitations of the TS 500 (2000) code. For C2 model, geometrical and mechanical safety limitations, such as the working stress in the nodal zones and the angle between the struts and ties, were considered based on the STM design suggestions in the literature and international design codes. Nevertheless, these suggestions were subsequently adapted to the local design instructions. Additionally, strength reduction factors of concrete and steel were considered to be 1.00 for the calculation of the specified strength values.

3.1 Conventional design approach

Because structural behavior of corbels is quite different with respect to traditional beams, calculation of load-bearing capacity and design of reinforcement layout are inherently distinctive. Shear strength of the corbel should firstly be checked with respect to the design shear force on the corbel. If this requirement cannot be satisfied, cross-sectional area might be enlarged or the concrete quality is increased.

Subsequently, cross-sectional areas of the reinforcements are determined. In this study, principal tensile reinforcement was calculated to be 254.0 mm^2 and selected as $2\phi8+2\phi10$ (257.6 mm^2) while horizontal web reinforcement was placed as closed stirrups of $4\phi6/40$ mm (226.2 mm^2) as seen in Fig. 3.

3.2 Integrated design approach

In particular, the whole member design approach based on the strut-and-tie model (STM) is currently recognized as the most rational and simplest method for designing shear critical structures (Chetchotisak *et al.* 2014). This method is a generalization of the truss analogy in which a structural continuum is transformed into a discrete truss with compressive forces being resisted by concrete and tensile forces by reinforcement. Being based on the lower bound theorem of plasticity (Kassem 2015), one early step in strut-and-tie modeling requires the user to envision a series of load paths within a structure (Hu *et al.* 2014).

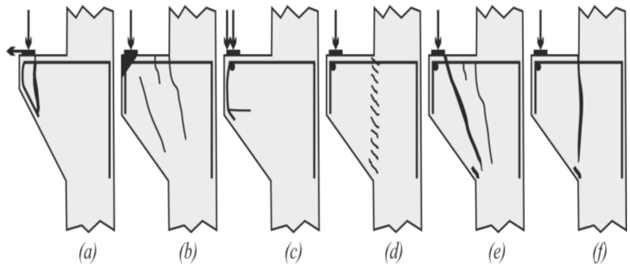

Fig. 1 Failure modes of reinforced concrete corbels

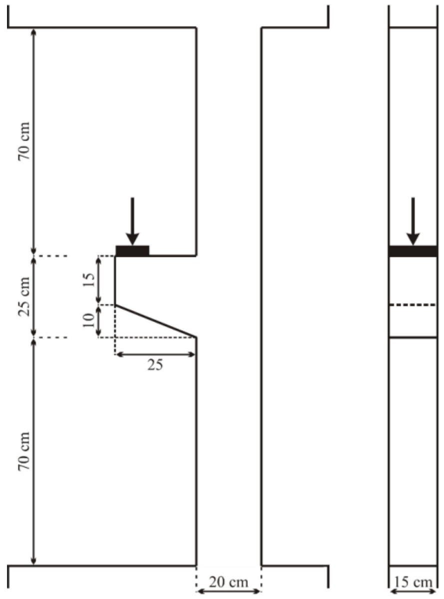

Fig. 2 Dimensions and loading details of the corbel model

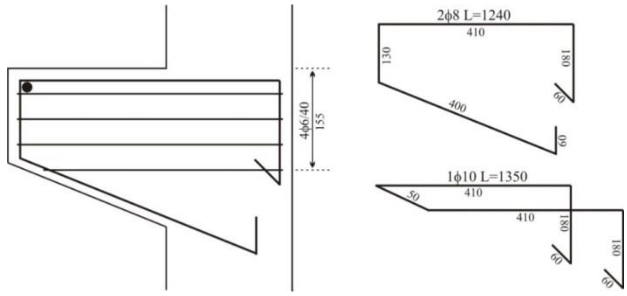

Fig. 3 Reinforcement details for C1 corbel (units in mm)

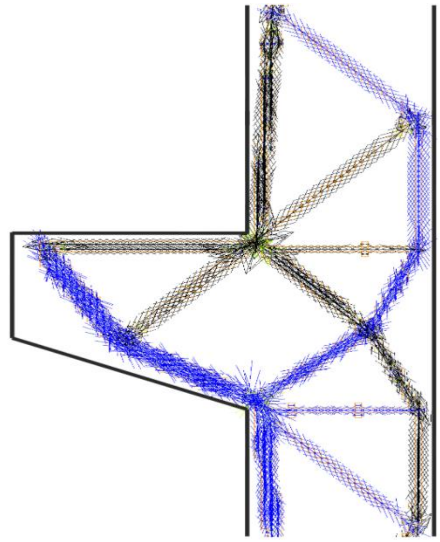

Fig. 4 Principal stress distribution for the optimal topology of the corbel (PI_{fsd}=9.185)

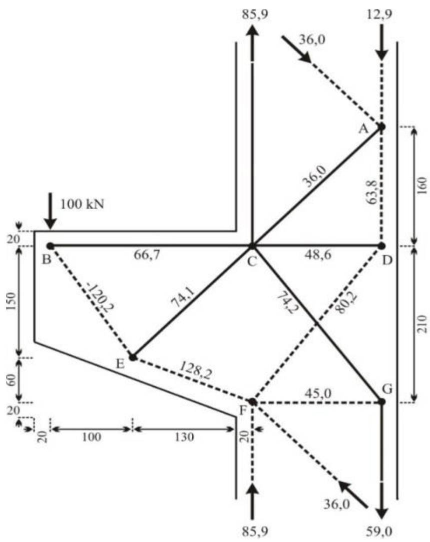

Fig. 5 Optimum strut-and-tie model of the corbel (units in kN and mm)

Since selection of a viable model from an unlimited number of possible solutions is a challenging task, especially in complex three-dimensional design domains with irregular cutouts (Yang *et al.* 2015), optimum reinforcement layout is determined by the assistance of topology optimization.

Topology optimization algorithm is established on the well-known evolutionary structural optimization method by Xie and Steven (1993). A wide variation of improvements have been applied on the method so far. The method is based on constructing the design domain of a structure by finite elements and iteratively analyzing the structure under given loads and support conditions. Sensitivity degree of each finite element is determined considering strain energy levels and a number of inefficient elements are removed from the design domain at every iteration. Inefficiency term here corresponds to contributing the structural performance at low levels in parallel with having low strain energy. Following this procedure, the stiffest structure resembling a truss at nearly fully stressed state is achieved. As it is encountered in all optimization algorithms, result of this iterative process is a local optimum. Optimal topology design is determined by means of a performance decision method considering stress levels, maximum displacement values and the amount of material to be used for the constitution of the internal truss.

Performance evaluation of yielded optimization results was firstly studied by Querin (1997). Subsequent studies of Zhao *et al.* (1998), Liang *et al.* (1999, 2000a, 2000b, 2001), Guan *et al.* (2001), Liang and Steven (2002), presented new performance evaluation approaches considering various structural behavior parameters. Alongside the previous studies, an improved performance index formulation, which is based on especially reinforced concrete structures (Özkal and Uysal 2010, 2012), was employed in order to lead

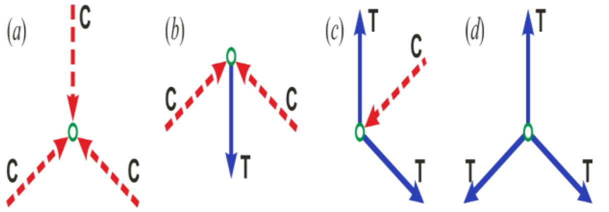

Fig. 6 STM node types: (a) CCC; (b) CCT; (c) CTT; (d) TTT

optimum reinforcement layout in this study. The performance index represented in this study is named as PI_{fsd} to demonstrate the effect of fully stressed design concept

$$PI_{fsd} = \frac{\left(\sigma_{0,max}^{vM} / \sigma_{0,avg}^{vM}\right) \cdot u_{0,max} \cdot W_0}{\left(\sigma_{i,max}^{vM} / \sigma_{i,avg}^{vM}\right) \cdot u_{i,max} \cdot W_i} \tag{1}$$

where $\sigma_{0,max}^{vM}$ and $\sigma_{i,max}^{vM}$ are the maximum von Mises stress values, $\sigma_{0,avg}^{vM}$ and $\sigma_{i,avg}^{vM}$ are the average von Mises stress values, $u_{0,max}$ and $u_{i,max}$ are the maximum displacement values, W_0 and W_i are the actual weight (or volume of the material) values of the initial and *i*th design domains.

Within the integrated design approach, topology optimization is applied to columns and corbel simultaneously. Fig. 4 shows a vectorial illustration of principal stress distribution for the optimum topology of the corbel and corbel-column connection regions that was tested in this study. Tension stresses are dominant in black sections, whereas compression stresses are dominant in blue sections. Truss form of the corbel's strut-and-tie model was constituted and analyzed in parallel with this topological design. Finally, the forces on the truss members were calculated, as shown in Fig. 5. Through the design procedure, required reinforcement amount and layout were first determined, and then safety verification processes were performed by adapting relevant construction codes to national instructions for the concrete struts, steel ties and nodal zones in the following order.

$$\text{Concrete struts:} \quad A_{c-i} \geq C_i / f_{cd} \tag{2}$$

$$\text{Steel tension rebar:} \quad A_{s-i} \geq T_i / f_{yd} \tag{3}$$

$$\text{Steel shear rebar:} \quad A_{sw-i} \geq T_i / f_{ywd} \tag{4}$$

$$\text{Nodal zones:} \quad a_i \geq \begin{cases} C_i / 1{,}00 f_{cd} b_w \text{ (CCC)} \\ C_i / 0{,}90 f_{cd} b_w \text{ (CCT)} \\ C_i / 0{,}70 f_{cd} b_w \text{ (CTT or TTT)} \end{cases} \tag{5}$$

$$a_i \geq \frac{C_i (0{,}8 + 170\varepsilon_1)}{f_{cd} b_w} \tag{6}$$

Where A_c, A_s and A_{sw} are cross-sectional areas of strut, tension rebar and shear rebar; *C* and *T* are strut force and tie force; f_{cd}, f_{yd} and f_{ywd} are design strength of concrete, steel tension rebar and shear rebar; *a* is the width of nodal face, b_w is the width of beam and ε_1 is the principal strain at the half height of the cross-section. Additionally, there are three

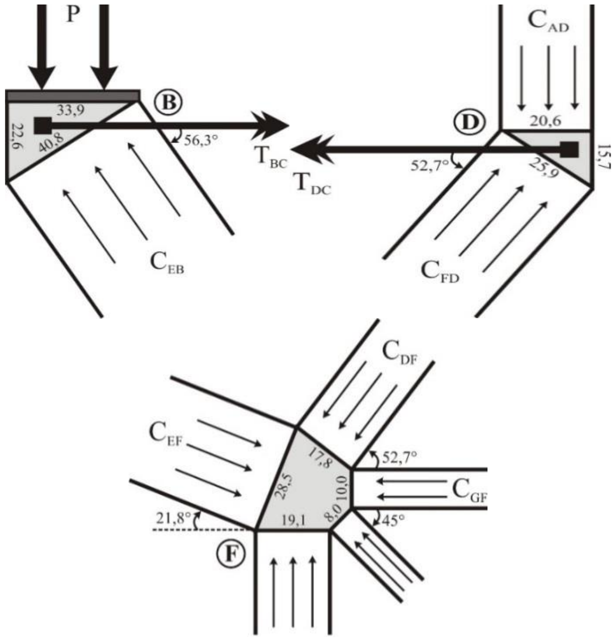

Fig. 7 Most critical nodal zones for strut-and-tie model of C2 corbel (units in mm)

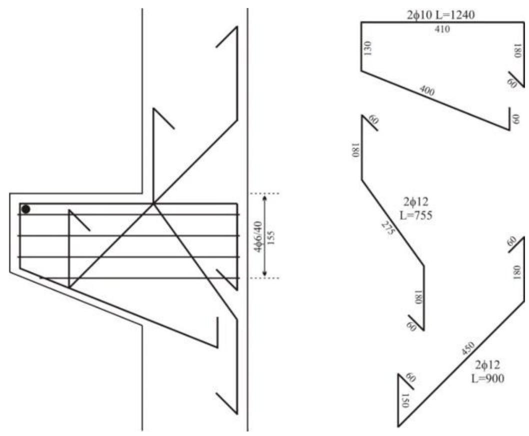

Fig. 8 Reinforcement details for C2 corbel (units in mm)

major node types as in most design specifications. For the denotation of nodes; *C* is for compression and *T* is for tension. A CCC node is bound by only struts while a CCT node anchors one tie, a CTT node anchors two or more ties and a TTT node is also possible without any strut (Fig. 6).

After those verifications, BC-CD and EC-CA ties were evaluated as continuous ties for the purpose of fitting ease and all of the reinforcements were calculated herein below.

F_{BC}=66667 N⇒A_{BC} =155.8 mm^2⇒Chosen: 2ϕ10 (157.1 mm^2)

F_{BC}=66667 N⇒A_{BC} = 155.8 mm^2⇒Chosen: 2ϕ10 (157.1 mm^2)

F_{CD}=48605 N⇒A_{CD}=113.6 mm^2⇒Chosen: 2ϕ10 (157.1 mm^2)

F_{EC}=74078 N⇒A_{EC} =173.1 mm^2⇒Chosen: 2ϕ12 (226.2 mm^2)

F_{CA}=36014 N⇒A_{CA} = 84.1 mm^2⇒Chosen: 2ϕ12 (226.2 mm^2)

F_{CG}=74214 N⇒A_{CG}=173.4 mm^2⇒Chosen: 2ϕ12 (226.2 mm^2)

To reduce the calculation time, safety verification processes were performed for struts and nodes simultaneously for each nodal zone. Bearing plate's width and concrete cover's height were determined according to the compression force values on the struts. Most critical nodal zones are presented in Fig. 7. Again for the purpose of fitting ease and considering friction-shear forces, closed stirrups were placed in the corbel to enclose longitudinal rebars of the columns same as C1 corbel. Relevant studies in the literature remark that vertical stirrups do not act effectively because of the corbel dimensions and it is suggested that horizontal stirrups parallel to the principal tensile stresses to be preferred and placed along the $2d/3$ depth from the corbel's top face. Reinforcement layout of C2 corbel is presented in Fig. 8.

As seen in Fig. 8, diagonal reinforcements corresponding to AE and CG ties, were bended at the edge-nodal zones and extended in the corbel and columns to provide sufficient adherence. Hooks are also established at the endings in order to increase the contribution of these reinforcements to the structural performance. Additionally an anchorage reinforcement was placed at the top corner of the corbel for the purpose of fitting ease. It has been selected as $1\phi10$ because anchorage reinforcement should not have a smaller diameter than the principal tension reinforcement.

4. Experimental setup

For the experimental stage of this study, ready-mixed concrete was used to produce two corbels at the same time. Concrete was predetermined to have a maximum aggregate radius of 15 mm, slump of 20 cm and compressive strength of 30 MPa. S420 and S220 construction steels were established as the reinforcing bars. Laboratory tests showed that the yield strength of the longitudinal reinforcements (ribbed $\phi8$, $\phi10$, $\phi12$ and $\phi16$) and stirrups (plain $\phi4$ and $\phi6$) were 428 MPa and 233 MPa, respectively.

Applied loads were measured by a two-way, flat-type load cell with a 250-kN capacity, whereas displacement values were measured using 100-mm displacement transducers. 5-mm strain gauges (SR*i*) were used to measure the strain of the steel reinforcements, and 30-mm strain gauges (SC*i*) were used to measure the strain on the face of the concrete. Calculations of the curvature at the beam-column connection regions were performed based on the strain values measured by these gauges. Yield moments of the test specimens were assumed to be reached at 75% of the maximum load while collapse moments were at 85% of the maximum load. In order to derive ductility coefficients, displacement ductility is the proportion of displacement value at the collapse moment to that at the yield moment. Flexural ductility is calculated in the same way using curvature values.

A loading program was applied according to the load values until the estimated system-yield value was reached. Between the yield and collapse moments, loading was performed according to the displacement of the corbel's end-point. To obtain curvature values and to draw flexural stiffness diagrams for the connection regions, 30-mm strain gauges were glued onto the columns' concrete faces by centering them at a distance of 5 cm from the corbel's top and bottom faces. In addition, 5-mm strain gauges were glued onto the reinforcements to provide a more suitable comparison and to determine contribution of the steel to total structural behavior. No data was collected from several of these gauges because they may have been damaged during concrete casting. Loading and measurement scheme of the test specimens (hydraulic cylinder, load cell, displacement transducer, strain gauges) are shown in Fig. 9.

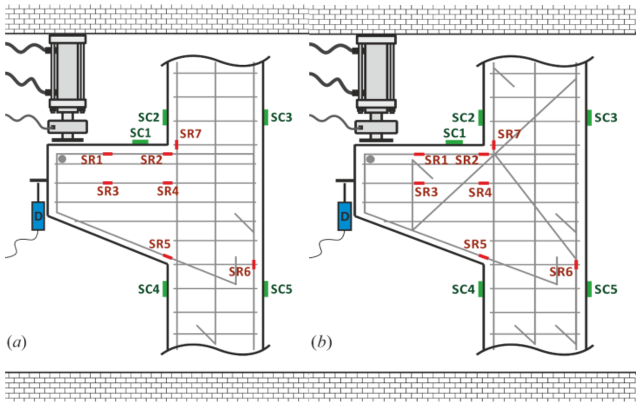

Fig. 9 Loading and measurement scheme of the test specimens: (a) C1; (b) C2

5. Experimental observation

When the load reached 65 kN for C1 specimen, a 45° degree inclined and 5 cm long crack occurred at top corner of the corbel. This crack bifurcated horizontally towards the column at 80 kN load and vertically downwards at 90 kN load. Initial cracks at upper column's interior side and lower column's exterior side, which are 5 cm long and have 10 cm between each of them, became thicker at 100 kN load. The most severe crack, which has occurred at 120 kN load and extending from just under the bearing plate into bottom corner of the corbel, became significantly enlarged and concrete strut crushed at 127.05 kN load in a brittle manner. Many new cracks occurred during the collapse moment. Loading was not stopped until the corbel cannot bear any more load and it has been noted that principal tensile reinforcements and closed stirrups were bended after concrete strut's crushing.

During the test for C2 specimen, first crack occurred at a load of 75 kN. Similar to the case of C1 specimen, this 3.5 cm long crack was nearly vertical and occurred at the top corner of the corbel. Two cracks at the upper column's interior side and another two cracks at the lower column's exterior side was seen at 90 kN load. Number of the horizontal column cracks increased after the 120 kN load level. In addition, another 45° degree inclined crack, which is perpendicular to the additional reinforcement in the column and lying from the exterior side of the column into the corbel's bottom corner, was recognized. At this moment, a vertical crack at the middle-top of the corbel became 12 cm long and extended as nearly 45° degree towards the bottom column. This crack enlarged and merged with a new crack, which started from the right side of the bearing plate.

(a) Collapse moment (b) Totally crushed (c) Scattered concrete was removed after the test

Fig. 10 Photographs for the test of C1 corbel

(a) Collapse moment (b) Totally crushed (c) Scattered concrete was removed after the test

Fig. 11 Photographs for the test of C2 corbel

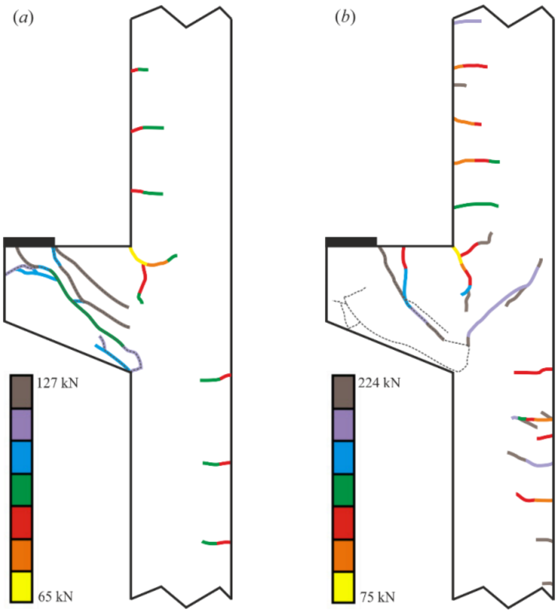

Fig. 12 Crack development of the test specimens: (a) C1; (b) C2

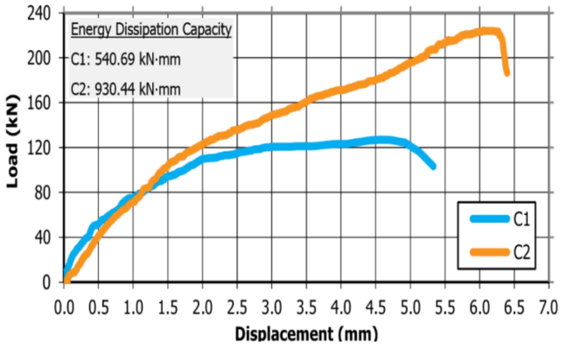

Fig. 13 Load-displacement graph of the test specimens

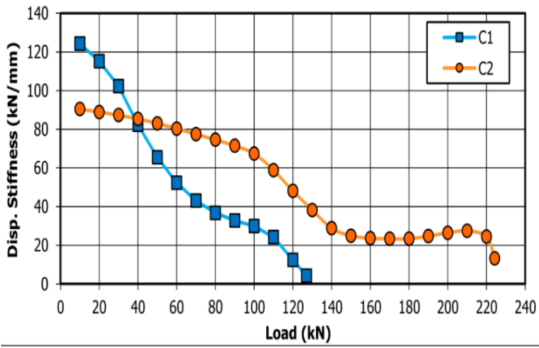

Fig. 14 Load-displacement stiffness graph of the test specimens

Corbel finally collapsed at 224.23 kN load following the crushing of the concrete strut. Despite the dramatic collapse of the corbel, load values did not drop rapidly and load level was nearly preserved while the vertical displacement of the corbel was increasing. Concrete cover and the concrete inside the corbel totally crushed and scattered following the continuation of loading.

Photographs that have been taken at the time of and after the collapse for both of the test specimens can be seen

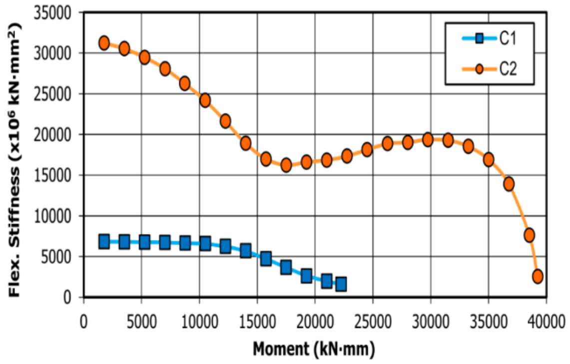

Fig. 15 Moment-flexural stiffness graph of the test specimens for the upper column's end-point

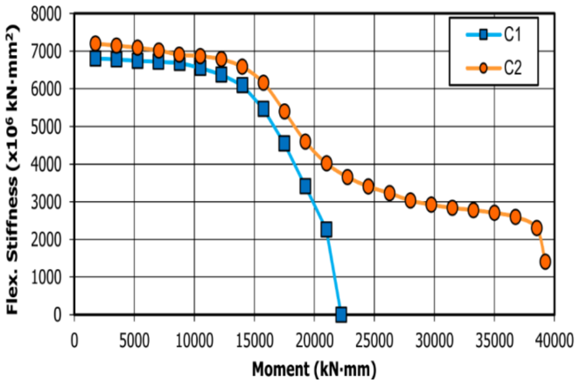

Fig. 16 Moment-flexural stiffness graph of the test specimens for the lower column's end-point

Table 1 Ductility coefficients for the test specimens

Test Specimen	Displacement Ductility	Flexural Ductility	
	Corbel's End-point	Upper Column's End-point	Lower Column's End-point
C1	3.26	1.75	1.60
C2	1.68	1.16	1.58

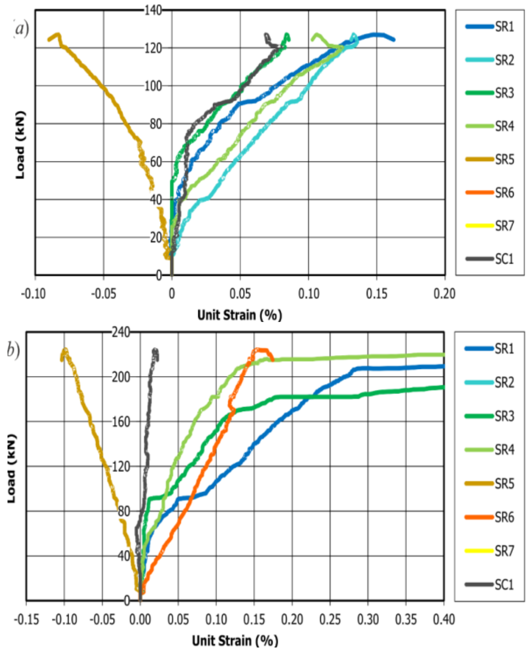

Fig. 17 Load-unit strain graph of the test specimens: (a) C1; (b) C2

in Figs. 10-11. Crack development drawings are also presented in Fig. 12. Both of the corbels resulted failure depending on the diagonal concrete strut's behavior. In spite of the splitting of C1 specimen's strut, diagonal reinforcements in the corbel and columns of C2 specimen prevented the splitting and provided simultaneous contribution of concrete strut with the principle and diagonal tensile reinforcements. Finally, reinforcements reached yield point as well as concrete strut crushed. Considering the crack development of the specimens, those diagonal reinforcements nearly enabled more uniform stress distribution (fully stressed state) in C2 specimen. C1 columns have less number of thicker cracks while C2 columns have more but thinner cracks.

6. Discussion of test results

Although total amount of steel reinforcement in the corbel and connection regions for C2 specimen is more than C1 specimen, equal amount of horizontal closed stirrups and less principal tensile reinforcement were used for STM design. Maximum bearable load for C2 specimen (224.23 kN) is nearly twice as C1 specimen (127.05 kN). Load-displacement and load-displacement stiffness graphs of the corbels are presented in Figs. 13-14. While the proportion of total energy dissipation values of the specimens is nearly 0.5, C2 specimen is again outstanding in terms of displacement stiffness values except the beginning part of the loading. C1 corbel has a higher initial displacement stiffness compared to C2 corbel. As well as the possibility of measurement glitches; authors think that total value of principal tensile reinforcement, which extends along the top of the corbel, might have led to that difference (C1: 257.61 mm^2, C2: 157.08 mm^2).

Graphs comparing the flexural stiffness values of the specimens are presented in Fig. 15 for the upper column, in Fig. 16 for the lower column. While the flexural stiffness values for the lower column of C2 specimen are consistently higher than C1 specimen, main difference arises for the upper column. Examination of the graph reveals that the flexural stiffness values of C2 specimen are very high since the beginning until the collapse. Following the cracks at the interior of upper column and at the exterior of lower column, flexural stiffness for the upper column of C2 specimen started to increase. Similar to the suggestions in the literature, optimization algorithm resulted in diagonal ties strengthening the connection of corbel and columns. Hence, the diagonal reinforcement, which connects the corbel and upper column, started to contribute more effectively to the whole system's structural performance after this moment and a stiffer behavior was observed for C2 specimen throughout the testing process.

According to the coefficient values of displacement and flexural ductility in Table 1, C2 specimen is less ductile than C1 specimen as expected. Owing to the geometry and intended purpose of construction of the corbels, these structural members are expected to have very small

Table 2 Unit strain values for the test specimens

ε (%) / P (kN)	C1 specimen SC1	SR1	SR2	SR3	SR4	SR5	SR6	SR7	C2 specimen SC1	SR1	SR2	SR3	SR4	SR5	SR6	SR7
20	0.001	0.000	0.005	0.000	0.000	-0.006	No Data!	No Data!	0.000	0.000	No Data!	0.002	0.001	-0.006	0.010	No Data!
40	0.007	0.004	0.024	0.000	0.007	-0.010			0.000	0.007		0.005	0.005	-0.010	0.026	
60	0.010	0.015	0.046	0.004	0.034	-0.022			0.000	0.014		0.005	0.012	-0.020	0.042	
80	0.017	0.035	0.070	0.026	0.056	-0.034			0.003	0.038		0.010	0.028	-0.026	0.059	
100	0.053	0.076	0.100	0.051	0.085	-0.052			0.007	0.091		0.043	0.036	-0.036	0.072	
120	0.077	0.120	0.127	0.081	0.124	-0.078			0.008	0.123		0.064	0.043	-0.045	0.087	
127.05	0.069	0.148	0.133	0.084	0.106	-0.083			0.009	0.136		0.074	0.048	-0.051	0.092	
140	-	-	-	-	-	-	-	-	0.010	0.150		0.084	0.057	-0.056	0.101	
160	-	-	-	-	-	-	-	-	0.011	0.182		0.107	0.071	-0.066	0.116	
180	-	-	-	-	-	-	-	-	0.013	0.219		0.174	0.093	-0.077	0.119	
200	-	-	-	-	-	-	-	-	0.014	0.269		0.606	0.118	-0.084	0.134	
220	-	-	-	-	-	-	-	-	0.018	1.018		1.262	0.413	-0.096	0.148	
224.23	-	-	-	-	-	-	-	-	0.019	1.649		1.405	0.670	-0.098	0.154	

displacement values under loading, not to present a ductile behavior. Both of the experiments show that the specimens collapsed by the crushing of the struts in the corbels. Unit-strain values of the reinforcements throughout the tests in Fig. 17 and Table 2 demonstrate that most of the reinforcements in C2 specimen reached their yield points unlike C1 specimen.

Most likely, concrete casting brought damage to several of the strain gauges on the specimens' reinforcement and these gauges provided no data. Examination of the unit-strain values of the reinforcements, reveals the contribution of the reinforcements to the total structural performance. As an exception, concrete strain at the top face of the corbels were recorded and C1 corbel was more stressed than C2 corbel. The biggest strain was observed on the principal tensile reinforcement (SR1) of C1 specimen, however, none of the reinforcements reached the yield point despite the collapse of the system. Nevertheless, reinforcements of C2 specimen generally reached to the yield point. Firstly, principal tensile reinforcement (SR1) and horizontal stirrup (SR3) yielded at their middle regions between 180 and 200 kN load moments. System was still bearing the increasing load even after yielding was recorded at the end region of the horizontal stirrup (SR4) at a load of 215 kN. It is obvious that reinforcements of C2 specimen worked more efficiently and higher bearing load was achieved in comparison with C1 specimen.

7. Conclusions

The strut-and-tie modeling method is used efficiently for the design and sizing of uncommon structural members in addition to the discontinuity regions that have complexity in the flow of internal forces. Nevertheless, the most important point for this method is that the designer requires adequate knowledge and experience. Otherwise, the process is not likely to yield designs with high performance, and critical design errors may arise.

In this study, reinforcement layout of a concrete corbel was designed by an integrated approach that consists of the topology optimization and strut-and-tie modeling methods. Another corbel was designed by the conventional method in order to carry out an experimental comparison based on their structural behaviors.

In addition to the improvement of maximum bearable load and stiffness values, the most challenging advantage of strut-and-tie modeling method on the tested models was observed that steel reinforcements served more effectively. Especially principal tensile reinforcements and horizontal stirrups passed over their yield points before the system's collapse. According to all of the studies in the literature and these experimental results, the new integrated design method presents more successful results than does the conventional method for the design of reinforced concrete members.

Because optimal truss system selection based on the determination of stress trajectories requires a specific level of design experience, it can be said that strut-and-tie modeling method is not very simple to apply single-handedly. However, as demonstrated in this study, the new integrated design method has an ability to assist the design engineers to increase structural performance in an easier way.

Acknowledgments

The research described in this paper was financially supported by the Scientific Research Projects Commission of Atatürk University (Grant no: BAP-2009/61).

References

AASHTO-LRFD (2010), *Bridge Design Specifications*, 5th Edition, Washington, U.S.A.

ACI 318M-14 (2014), *Building Code Requirements for Structural Concrete and Commentary*, Michigan, U.S.A.

Bendsøe, M.P. and Kikuchi, N. (1988), "Generating optimal topologies in structural design using a homogenization method", *Comput. Meth. Appl. Mech. Eng.*, **71**(2), 197-224.

BS 8110 (1997), *Part 1, Code of Practice for Design and Construction*, London, U.K.

Celep, Z. and Kumbasar, N. (2005), *Betonarme Yapılar*, Beta Press, İstanbul, Turkey.

Chae, H.S. and Yun, Y.M. (2015), "Strut-tie model for two-span continuous RC deep beams", *Comput. Concrete*, **16**(3), 357-380.

Chetchotisak, P., Teerawong, J., Yindeesuk, S. and Song, J. (2014), "New strut-and-tie-models for shear strength prediction and design of RC deep beams", *Comput. Concrete*, **14**(1), 19-40.

Collins, M.P. and Mitchell, D. (1986), "Rational approach to shear design-the 1984 Canadian code provisions", *ACI J. Proc.*, **83**(6), 925-933.

Cook, W.D. and Mitchell, D. (1988), "Studies of disturbed regions near discontinuities in reinforced concrete members", *ACI Struct. J.*, **85**(2), 206-216.

CSA A23.3-04 (2004), *Design of Concrete Structures*, Ontario, Canada.

Eurocode 2 (2004), *Design of Concrete Structures-Part 1-1:*

General Rules and Rules for Buildings (EN 1992-1-1), Brussels, Belgium.

FIB Model Code 2010 (2010), *The Fib Model Code for Concrete Structures*, Lausanne, Switzerland.

Guan, H., Chen, Y.J. and Loo, Y.C. (2001), "Topology optimization of bridge type structures with stress and displacement constraints", *J. Comput. Eng. Sci.*, **2**(2), 199-221.

Hu, Q.N., Ley, M.T. and Russell, B.W. (2014), "Determining efficient strut-and-tie models for simply supported beams using minimum strain energy", *ACI Struct. J.*, **111**(5), 1015-1025.

Hwang, S.J., Lu, W.Y. and Lee, H.J. (2000), "Shear strength prediction for reinforced concrete corbels", *ACI Struct. J.*, **97**(4), 543-552.

Kassem, W. (2015), "Strength prediction of corbels using strut-and-tie model analysis", *J. Concrete Struct. Mater.*, **9**(2), 255-266.

Kriz, L.B. and Raths, C.H. (1965), "Connections in precast concrete structures-strength of corbels", *PCI J.*, **10**(1), 16-61.

Liang, Q.Q. and Steven, G.P. (2002), "A performance-based optimization method for topology design of continuum structures with mean compliance constraints", *Comput. Meth. Appl. Mech. Eng.*, **191**(13-14), 1471-1489.

Liang, Q.Q., Xie, Y.M. and Steven, G.P. (1999), "Optimal selection of topologies for the minimum-weight design of continuum structures with stress constraints", *J. Mech. Eng. Sci.*, **213**(8), 755-762.

Liang, Q.Q., Xie, Y.M. and Steven, G.P. (2000a), "Optimal topology selection of continuum structures with displacement constraints", *Comput. Struct.*, **77**(6), 635-644.

Liang, Q.Q., Xie, Y.M. and Steven, G.P. (2000b), "Optimal topology design of bracing systems for multistory steel frames", *J. Struct. Eng.*, **126**(7), 823-829.

Liang, Q.Q., Xie, Y.M. and Steven, G.P. (2001), "A performance index for topology and shape optimization of plate bending problems with displacement constraints", *Struct. Multidiscipl. Optim.*, **21**(5), 393-399.

MacGregor, J.G. (1997), *Reinforced Concrete Mechanics and Design*, 3rd Edition, Prentice-Hall International Inc., New Jersey, U.S.A.

Mattock, A.H., Chen, K.C. and Soongswang, K. (1976), "The behavior of reinforced concrete corbels", *PCI J.*, **21**(2), 52-77.

Michell, A.G.M. (1904), "The limits of economy of material in frame-structures", *Philos. Mag.*, **8**(47), 589-597.

Mörsch, E. (1902), *Concrete-Steel Construction (Der Eisenbetonbau)*, 3rd Edition, McGraw-Hill Book Company, New York, U.S.A.

NZS 3101-1 (2006), *Concrete Structures Standard: Part 1-The Design of Concrete Structures*, Wellington, New Zealand.

Özkal, F.M. (2012), "Design and experimental verification of the optimum reinforcement layout for reinforced concrete members with the aid of topology optimization and strut-and-tie modeling methods", Ph.D. Dissertation, Atatürk University, Turkey.

Özkal, F.M. and Uysal, H. (2010), "A new performance index formulation aiming to attain fully stressed designs for topology optimization problems", *Sci. Res. Ess.*, **5**(15), 2027-2036.

Özkal, F.M. and Uysal, H. (2012), "A fully stressed design method to determine the optimum strut-and-tie model for beam-column connections", *Int. J. Comput. Methods*, **9**(3), 1250035.

Özkal, F.M. and Uysal, H. (2016), "A computational and experimental study for the optimum reinforcement layout design of an RC frame", *Eng. Comput.*, **33**(2), 507-527.

Qazi, S., Miche, L., Ferrier, E. and Limam, A. (2015), "Strut-and-tie model for a reinforced concrete wall strengthened with carbon fibre-reinforced polymers", *Compos. Struct.*, **128**, 87-99.

Querin, O.M. (1997), "Evolutionary structural optimisation: Stress based formulation and implementation", Ph.D. Dissertation, University of Sydney, Australia.

Ritter, W. (1899), "Die bauwise hennebique", *Shweizer. Bauzeit.*, **33**(7), 59-61.

Russo, G., Venir, R., Pauletta, M. and Somma, G. (2006), "Reinforced concrete corbels-shear strength model and design formula", *ACI Struct. J.*, **103**(1), 3-10.

Schlaich, J., Schaefer, K. and Jennewein, M. (1987), "Toward a consistent design of structural concrete", *PCI J.*, **32**(3), 74-150.

TS 500 (2000), *Requirements for Design and Construction of Reinforced Concrete Structures*, Ankara, Turkey.

Victoria, M., Querin, O.M. and Marti, P. (2011), "Generation of strut-and-tie models by topology design using different material properties in tension and compression", *Struct. Multidiscipl. Optim.*, **44**(2), 247-258.

Wang, S.Y., Wang, M.Y. and Tai, K. (2006), "An enhanced genetic algorithm for structural topology optimization", *J. Numer. Meth. Eng.*, **65**(1), 18-44.

Wight, J.K. and Parra-Montesinos, G.J. (2003), "Strut and tie model for deep beam", *Concrete*, **25**(2), 63-70.

Xie, Y.M. and Steven, G.P. (1993), "A simple evolutionary procedure for structural optimization", *Comput. Struct.*, **49**(5), 885-896.

Yang, Y., Moen, C.D. and Guest, J.K. (2015), "Three-dimensional force flow paths and reinforcement design in concrete via stress-dependent truss-continuum topology optimization", *J. Eng. Mech.*, **141**(1), UNSP 04014106.

Yavuz, G. (2016), "Shear strength estimation of RC deep beams using the ANN and strut-and-tie approaches", *Struct. Eng. Mech.*, **57**(4), 657-680.

Zhao, C., Hornby, P., Steven, G.P. and Xie, Y.M. (1998), "A generalized evolutionary method for numerical topology optimization of structures under static loading conditions", *Struct. Optim.*, **15**(3-4), 251-260.

CC